Digest Journal of Nanomaterials and Biostructures Vol. 6, No 2, April - June 2011, p. 809 - 818

DEVELOPMENT AND CHARACTERIZATION OF POLY(VINYL ALCOHOL) MATRIX FOR DRUG RELEASE

A. ROGOJANU*, E. RUSU[a], N. OLARU[a], M. DOBROMIR, D.O. DOROHOI
"Al. I. Cuza" University, Faculty of Physics, Iasi, Romania
[a]*Institute of Macromolecular Chemistry "Petru Poni", Iasi, Romania*

Properties of the PVA/SA system as films or nanofibres have been assessed through the combined use of Attenuated Total Reflectance Fourier Transform Infrared (ATR FTIR) spectroscopy, X-ray photoelectron spectroscopy (XPS), scanning electron microscopy (SEM) measurements. The release behaviour of SA from films and nanofibres was also investigated. The properties of poly(vinyl alcohol)/SA systems were presented in comparison with those of neat polymer.

(Received March 21, 2011; Accepted April 21, 2011)

Keywords: poly(vinyl alcohol), nanofibres, salicylic acid, drug release

1. Introduction

At about hundred years since when polyvinyl alcohol (PVA) was obtained by Hermann and Haehnel this polymer is in the top of polymers from point of view of academic researchers, end users interest and market demand. Its excellent films, fibres and hydrogels forming, emulsifying and adhesive properties, solublility in water, biodegradability, combined with its semicrystalline character, ability to form hydrogen bonding and versatility to be functionalized in bulk and at surface make it an ideal choice as adhesive, paper coatings, ceramic binder, textile wrap sizing, polarizers and optical filters, membranes with selective permittivity etc.

Thus PVA meet the needs of today's sustainability requirements for consumer from numerous fields including food, agriculture, chemical, pharmaceuticals, textiles, cosmetics, medical etc. Large quantities of PVA are manufactured to cover the variation of the demands. It is commercially available in a broad range of degrees of polymerisation and hydrolysis [1]. Taking into account the PVA properties, it was expected that this polymer as matrix to be found a developing niche in nanotechnology. The different type of nanomaterials - nanoparticles or clusters, nanolayers or nanofilms, nanofibres and nanodots have been proved to be optimal candidates for many important applications in medicine, industry and agriculture. Most of polymer and composite fibres with nanoscale diameters were produced by electrospinning process based on the uniaxial stretching of a viscoelastic jet derived from a polymer solution, gel or melt under electrostatic force [2]. The fibres obtained via electrospinning are assembled as a three dimensional structured fibrous membrane with controllable pore structure and high specific surface area. The very small diameter of nanofibres, their high surface area to volume, small inter-fibrous pore size, superior mechanical performance, versatility of design make them enable for development of advanced materials [3, 4]. The usage of polymeric water based systems as spinning media is preferable for an environmentally acceptability [5]. The applications of electrospun fibres include multifunctional membranes, biomedical structural elements, protective shields in speciality fabrics, filter media for submicron particles in the separation industry, composite reinforcement [3, 6, 7, 8, 9, 10].

* Corresponding author: rogojanu_alina@yahoo.com

The polyvinyl alcohol (PVA) is an adequate spinning material because it meets specific demands on the nanofibres as their environmentally friendly production. Many reports related to researches and developments in the field of the polymer films and nanofibres including processing, structure, functionalization, properties characterization, applications, and modelling and simulations are presented in the literature [11].

The idea of incorporating nanoscale fillers into polymer solution has been extended to prepare a composite solution of organic and inorganic materials for film casting and nanofibres electrospinning. Kenawy has explored electrospun fibres/tetracycline hydrochloride as drug delivery system. This achievement has started the interest of researches toward potential biomedical applications of the electrospun fibres [3, 4, 12].

PVA has been used as matrix for preparation of films polarizers by incorporation of iodine or dichroic dyes [13, 14]. PVA films and nanofibres have found wide applications in membrane technologies [15], preparation of biomedical materials (dialysis membranes, wound dressing, artificial skin, cardiovascular devices and systems that release active substances in a controlled manner) [16, 17]. It is expected that the compound-loaded electrospun fibre to exhibit much better release characteristics than cast films both in terms of the total amount and the rate of release of the drugs [9]. The electrospun fibre mats has a porous structure that offers greater surface area that would, it is assumed, allow the drug molecules to diffuse out from the matrix much more conveniently unlike as-cast films characterized by dense structure [3].

Salicylic acid (SA) belongs to aromatic carboxylic hydroxy acid class. Their name is often associated with the aspirin used as analgesic, antipyretic and as anti-inflammatory drug [18]. SA exhibit anti-fungal, anti-bacterial, anti-viral action. It can be used as a disinfectant and keratolic agent (acnee drugs) [19, 20]. Taking into account all these we focused on the obtaining of films and nanofibres from polyvinyl alcohol containing SA and the investigation of their characteristics.

2. Experimental

2.1. Materials

The poly(vinyl alcohol) (PVA) with average molecular weight M_w= 39600 was supplied from the Chemical Plant Râşnov. The polymer was amorphous and atactic. The tacticity of poly(vinyl alcohol) was estimated taking into account the ratio of the absorption bands at 917 and 850 cm^{-1} from FTIR spectra [21]. Salicylic acid, disodium hydrogen phosphate and sodium dihydrogen phosphate (Sigma Aldrich) were used as received. The solvents used were distilled water, for preparation of polymer solution and ethanol for the dissolution of salicylic acid.

2.2. Methods

A weighed amount of partially hydrolyzed PVA was dissolved in pure water and heating gently, to 70-80 ^oC in a water bath to prevent thermal decomposition of polymer. Then, the clear viscous solution (about 10%) was left to cool at room temperature and subsequently it was filtered and degassed in an ultrasonic bath. The salicylic acid, dissolved in ethanol was mixed with PVA solution, maintained at constant temperature of 25 ^oC under stirring at 300 rpm for one hour. The mixture with desired content of salicylic acid was filtered and then was used for preparation of the films and nanofibres. The films obtained by casting method on a flat glass plate were further dried in air for 3 days and then in a desiccator at room temperature. The solution of PVA neat and with salicylic acid entrapped on were electrospun with feeding rate 0.5 mL/h when 25 kV was applied with tip-to-collector distance, about 15 cm. A rotating metal drum was used to collect the resulting fibre to give a white sheet of non-woven fibre. The process was carried out in air at room temperature. The initial weight of the drug incorporated in the electrospun and films samples are presented in table 1 (P1-4 – films, N1-4 – nanofibres).

Table 1. The initial weight of the drug loaded in the polymer samples.

Sample	PVA weight (g)	salicylic acid weight(g)
P1, N1	2	-
P2, N2	2	$0.625 \cdot 10^{-3}$
P3, N3	2	$0.812 \cdot 10^{-3}$
P4, N4	2	$1.187 \cdot 10^{-3}$

2.3. Preparation of phosphate buffer solution

In vitro dissolution studies are performed at 5.5 pH of the skin. The stock solutions (a) and (b) were prepared by dissolving 1.1186 g disodium hydrogen phosphate in 100 ml distilled water and 0.9112 g sodium dihydrogen phosphate in 100 ml water respectively. The phosphate buffer solution (pH 5.5) was prepared by mixing 144.15 ml stock solution (a) with 5.85 stock solution (b). The pH solution can be adjusted using 0.1 N hydrochloric acid if is necessary.

2.4. Measurements

FT IR spectral measurements were performed using a Bruker Vertex 70 spectrometer. For each spectrum, the average of 100 successive scans, over the range of 400–4000 cm^{-1} with a resolution of 2 cm^{-1} was recorded. Software OPUS 6.0 (BRUKER) was used for data processing, which was baseline corrected by rubber band method with CO_2 bands excluded. The entire spectra were normalized.

The UV spectra of solutions containing salicylic acid released from films and electrospun nanofibres samples were acquired using SPECORD M42 Carl Zeiss Jena spectrophotometer in a matched pair of 10 mm quartz cells.

The SA release testing were made by submerging 20 mg of film and nanofibres mats, respectively, in 10 mL buffer solution. At a specified period ranging between 0 and 120 h, 3 ml of the buffer solution was withdrawn and replaced with the same volume of fresh buffer solution. To estimate the concentration of the released SA from the samples it was drawn the calibration curve in buffer (pH 5.5). 5 mg of salicylic acid was dissolved in 100 mL of buffer to obtain the working standard solution of 50 μg/mL. Aliquots of 1 ml to 15 ml from the stock solution were transferred to 20 mL volumetric flask and the volume was adjusted to 20 mL with the solvent. The measurements were carried out in the UV range, at the wavelength of 297 nm where the SA spectrum presents a maximum, against the blank solution prepared in the same manner without adding the salicylic acid. The curves were fit to a straight line according to an equation $A=0.02795\ C + 0.05697$, where C is the concentration of SA (in μg/mL) in the solution and A is the absorbance at 297 nm measured in a 1 cm quartz cell (correlation coefficient: $r^2 = 0.99833$). The absorbance of each solution has been measured and based on the calibration curve and the SA concentration was evaluated. The percentage of the released drug in duplicate samples was then calculated based on the initial weight of the drug incorporated in the electrospun and films samples.

The X-Ray photoelectron spectroscopy (XPS) used to study the surface structure of the polymer films was performed on PHI 5000 Versa Probe X-ray photoelectron spectrometer equipped with a conventional hemispherical analyser. The X-ray employed was a monochromatized Al Kα (1486.7 eV) source operating at 24.2 W. The analysis area was 0.1 mm^2 (100 μm×100 μ m) using a take-off angle of 45^o relative to the surface normal. The measurements were carried out in a vacuum atmosphere (around 10^{-7} Pa). The binding energy scale was corrected for static charging, using an electron binding energy, of 285.0 eV for the C1s level of aliphatic hydrocarbons.

Scanning electron microscopy (SEM) analysis of nanofibres was performed using a Tescan Vega II SBH instrument. The microscope is entirely operated by computer and contains an

electron gun with tungsten filament at an acceleration voltage 30 KV. Images were taken from the most relevant aspects.

3. Results and discussion

PVA electrospun fibres and films obtained from polymer solution were uniform. It was observed that the films are transparent while the electrospun mats are opaque due to light scattering from the fibrous structure. The dimensional measurements revealed that the electrospun fibre sheets and films thickness were of about 10 μm and 100 μm, respectively.
The structural features of the samples have been successfully ascertained by a technique versatile and accessible for the study of the polymers, FT IR spectroscopy, in the range 4000–600 cm^{-1}. These are presented in figure 1.

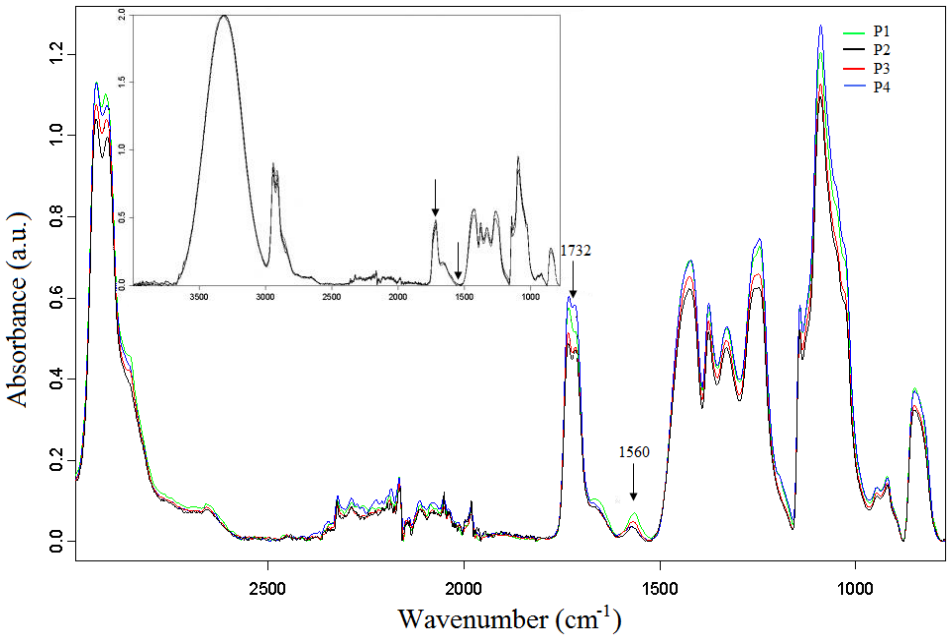

Fig. 1. Difference in the ATR-FTIR spectra of the films (main) and nanofibres (inset);

All FTIR spectra exhibit the characteristic absorption bands typical of poly (vinyl alcohol) which can be assigned to vibrations of the C=O, C–H, C–OH, C–O bonds [22]. For film and fibre samples under study it can be noticed that some observable changes in the intensity and frequency of the bands appear in their spectral features. The PVA film samples give very strong and slightly broad band centred at about 3295 cm^{-1} as the stretching vibration of OH group. This indicates presence both of the strong hydrogen bonding as intra- and/or intertype and the free hydroxyl groups. The hydroxyl groups from residual water contribute also to this band. In the region (2800-3000 cm^{-1}) both the CH_2 symmetric (ν_s) and antisymmetric(ν_{as}) stretching vibration bands are particularly notable [23]. The position of the antisymmetric and symmetric CH_2 stretching vibration bands at 2915.5 and 2854 cm^{-1}, suggests that the hydrocarbon chains of polymer takes a *trans* zigzag conformation [24, 25]. The residual acetate groups, resulted from manufacturing, handling, and degradation of the polymer [26, 27] exhibited peaks at about 2940 cm^{-1} assigned to methyl groups. At 1732 cm^{-1} and 1716 cm^{-1} (antisymmetric and symmetric C=O stretching), 1376 cm^{-1} (C–H wagging), 1258 cm^{-1} (C–O bending) appear bands from the same groups. Other stretching vibrational bands appear at 1650 and 1560 cm^{-1} for C=O and C=C groups. Otherwise these observations related to C=O and C=C groups are in good agreement with those by UV spectroscopy as was reported in literature [28, 29, 30]. The band which appears at 1732 cm^{-1} in the spectra of film samples become shoulder in the case of electrospun fibres, while the band about

1560 cm^{-1} appears only in the spectra of films. The low-frequency bands in the IR spectra of the samples belong to the stretching vibrations of associated C=O groups engage in a hydrogen bond with the OH groups. The disappearance of band at 1560 cm^{-1} from the spectra of electrospun fibres can be associated with crosslinking of C=C linkages. In complement to C–H stretching vibration, the C–H deformation bands appear at about 1420 cm^{-1} (CH_2) and 1328 cm^{-1} ($C–CH_3$). At 1142 cm^{-1} a peak, assigned as C–C and C–O–C stretching vibrations correlated to the polymer crystallinity appears and it seems to exhibits same tendency as other bands from the spectra. On observe a sharp absorption band suggesting that PVA is a semicrystalline polymer. The bands at about 1375 cm^{-1} and 1090 cm^{-1} due to C-O-H bending and C–O stretching coupled with O–H bending vibrations, respectively exhibit the same behaviour. The position of CH_2 bands at 917 cm^{-1} and 850 cm^{-1} revealed the presence of the PVA atactic form [31, 32].

Further characterization of films samples was performed by XPS analysis. The XPS measurements provided valuable information for various functional groups at films surface. The photo peaks consistent with the types and relative concentrations of the elements are present. To verify the chemical changes underwent on the PVA surface, XPS resolution spectra for both the neat and SA loaded PVA films were taken. In order to clarify what functional groups are on polymer film surface and to estimate their relative amounts, deconvolution procedure was performed on the C1s and O1s XPS spectra. Gaussian function was used to curve fit. Every peak was labelled numerically and the binding energy corresponding to each peak was used to identify the chemical functional groups in the sample. The XPS C1s core-level spectrum of original PVA four carbon peaks which was associated with the hydrocarbon atoms C1 (C-C/C-H), the methylene carbon singly bonded to oxygen C2 (C–O/C-OH), carbonyl carbon C3 (C=O) and the ester carbon atoms C4 (O–C=O/$COOCH_3$), respectively, as shown in Figure 2.

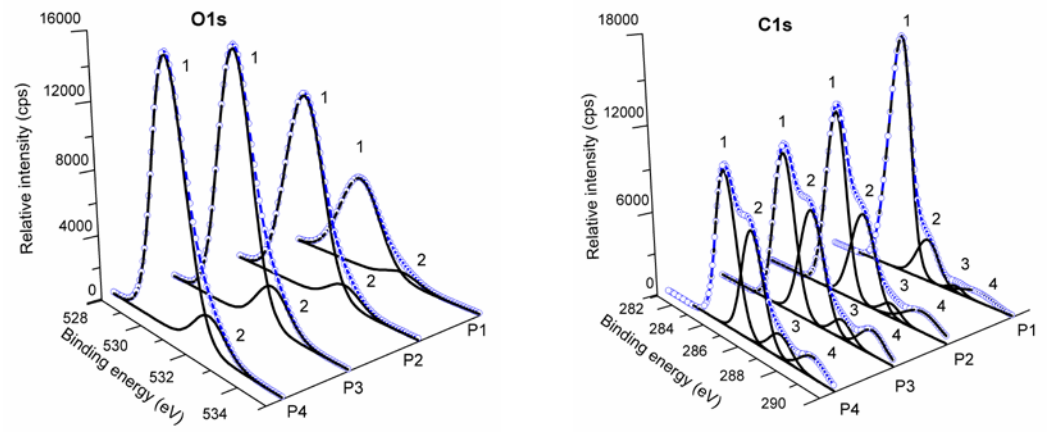

a) b)

Fig. 2. High resolution XPS spectra of (a) O1s and (b) C1s peaks for films samples; ○- original curve; solid line - fitted curve.

It can be seen from C1s and O1s spectra in Figure 2(a, b) that the size of the peaks vary with amount of drug loaded in PVA films. The bond energies associated with hydroxyl functional groups of PVA (C–OH), characteristic to this polymer can be identified at 286.1 eV and 531.0 eV, respectively in the C1s and O1s spectra. The final two C1s components at 287.6 eV and 288.8 eV were attributed to carboxyl and carbonyl species resulting from incomplete alcoholysis of PVA. This fact is in agreement with ATR FTIR results.

The surface composition was obtained from measurement of the areas of the peaks from C1s and O1s spectra. According to table 2, the surface modification of PVA was confirmed. Incorporation of SA in PVA matrix generates changes in distribution of functional groups at samples surface. The data presented in table 2 revealed the trend of the percentage of peak C1s, which decreases when the content in SA increases. The variation of O/C ratio indicates the polar groups reorientation along polymer chains or/and at end chains of polymer at surface of film. The SA represents a possible agent favouring hydrogen bonds and in PVA matrix it can intercalate

between polymer chains. Thus some interchain H bonds are disrupted and near of surface the OH groups are forced to move outwards on the PVA surface.

Table 2. Surface chemical compositions for PVA samples

Functional groups	Binding energy (eV)	Composition %			
		P1	P2	P3	P4
C-C/CH	284.8	54.96	40.57	35.02	32.87
C-O/COH	286.1	38.79	50.87	53.83	54.53
C=O	287.6	3.36	4.73	7.30	8.13
O-C=O/ $COOCH_3$ and COOH	288.8	2.87	3.80	3.82	4.45

In terms of nanofibres was of interest to investigate their geometric properties such as fibres diameter, diameters distribution, fibres orientation and in this sense scanning electron microscopy (SEM) was used. The electrospun mats were sputtered with a thin layer of gold prior to SEM observation. In figure 3 is shown the SEM micrographs and fibres diameters distribution for all nanofibres samples. One of the most important features related with electrospun fibres is their diameter.

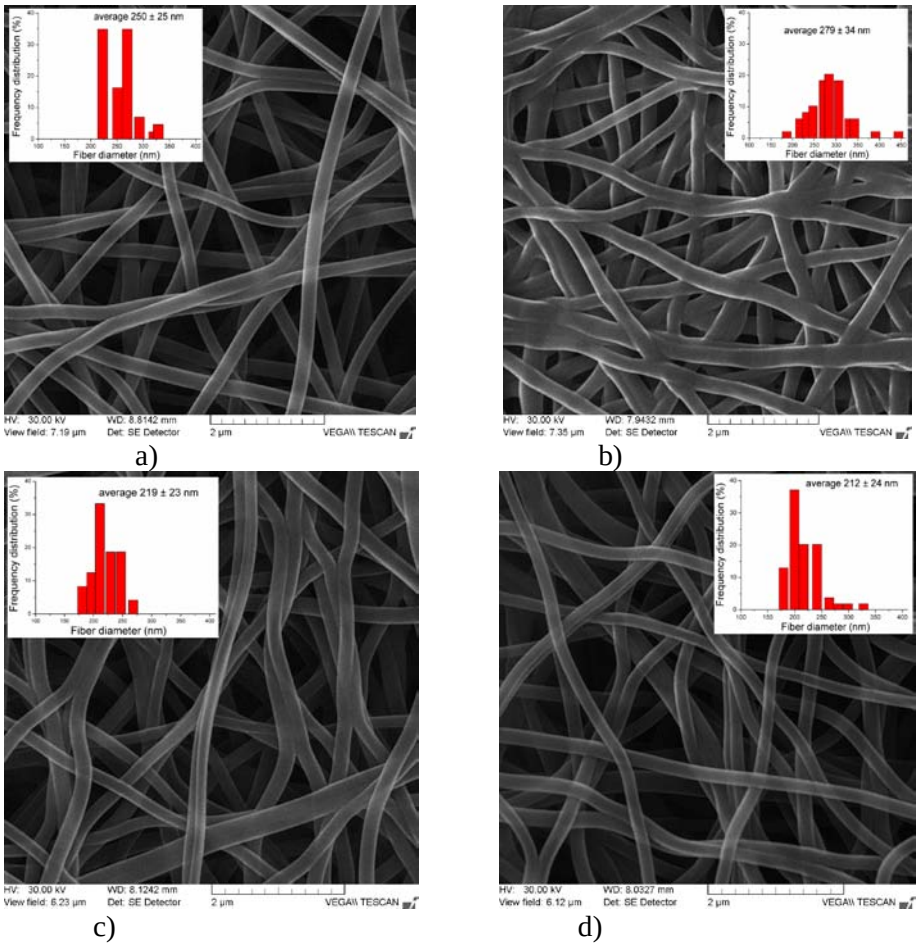

Fig. 3. SEM micrographs and fibres diameters distribution of a) N1; b) N2; c) N3; d) N4 samples

For statistical analysis, image processing software ImageJ (NIH, USA) was used to measure the nanofibres diameters from SEM micrographs. The average diameter was obtained by measuring at 50 individual nanofibres. For each fibre, the multiple measurements of diameters were achieved to see if the fibres are uniform. As is presented in figure 3, PVA electrospun fibres smooth, uniform and bead-free were obtained from polymer solution. No SA crystals were detected by SEM on the surface of the fibres. This indicated that, SA was totally embedded in the fibres. The individual electrospun fibres appear to be randomly distributed and generally had similar thickness along the fibre. It was also found that the fibres became finer when the amount of drug increase. The fibres diameters ranged from 212 to 279 nm.

The in-vitro drug release studies were performed at temperature 37 ^{o}C and pH value of 5.5, which simulated the skin pH. The experiments were carried out in duplicate and the results were reported as average values. The graphs of salicylic acid release in a function of time were created on the basis of the obtained results and are presented in figure 4.

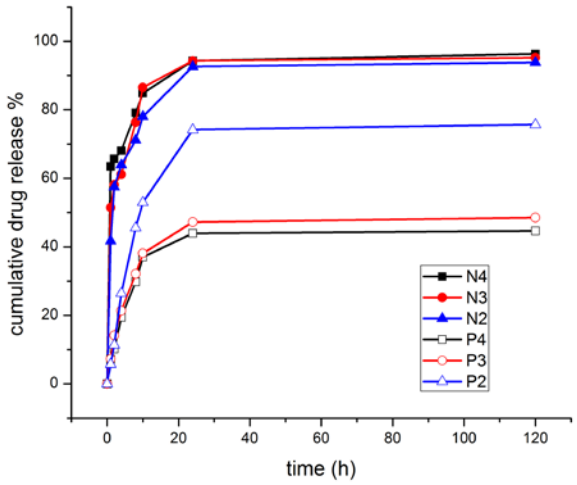

Fig. 4. In-vitro drug release profile of SA from drug polymer matrix.

The amounts of SA released from all samples of the SA loaded PVA increase very rapidly over the first 10 h; after this period they increase gradually until reaching equilibrium. From the cumulative release studies of SA-PVA films it was observed that within the first hour 5-7.5% of the total release occurred, whereas in the case of SA loaded electrospun fibres approximately 40-65% of the total drug release of SA occurred in releasing medium.

The mechanism by which drugs are released requires dissolution of the drugs followed by diffusion through the swelling porous structure to reach the release medium, usually water or a pH buffer solution for in vitro studies. When the concentration of SA increases, the drug becomes trapped on the surface of the polymer matrix during the drying and storage steps of samples. Migration of drug may result in a heterogeneous distribution of drug in the polymer matrix and lead to burst release. This behaviour may be the optimal mechanism of delivery in several instances [33, 34]. The burst phenomenon that happened in many cases was partly due to the formation of pores, the migration of drugs towards the sample surface with water convection during the drying and storage process [35, 36]. An increased removal rate of the organic solvent causes an increase in porosity of the matrices and this fact can explain the release behaviour of nanofibres vs. film samples. In order to study the SA release from the PVA films and nanofibers, various mathematical models [37] can be used to analyze the experimental data (figure 5). These models provide information on release kinetics and transport processes. Criteria for selecting the most appropriate model were based on coefficient of correlation shown in table 3.

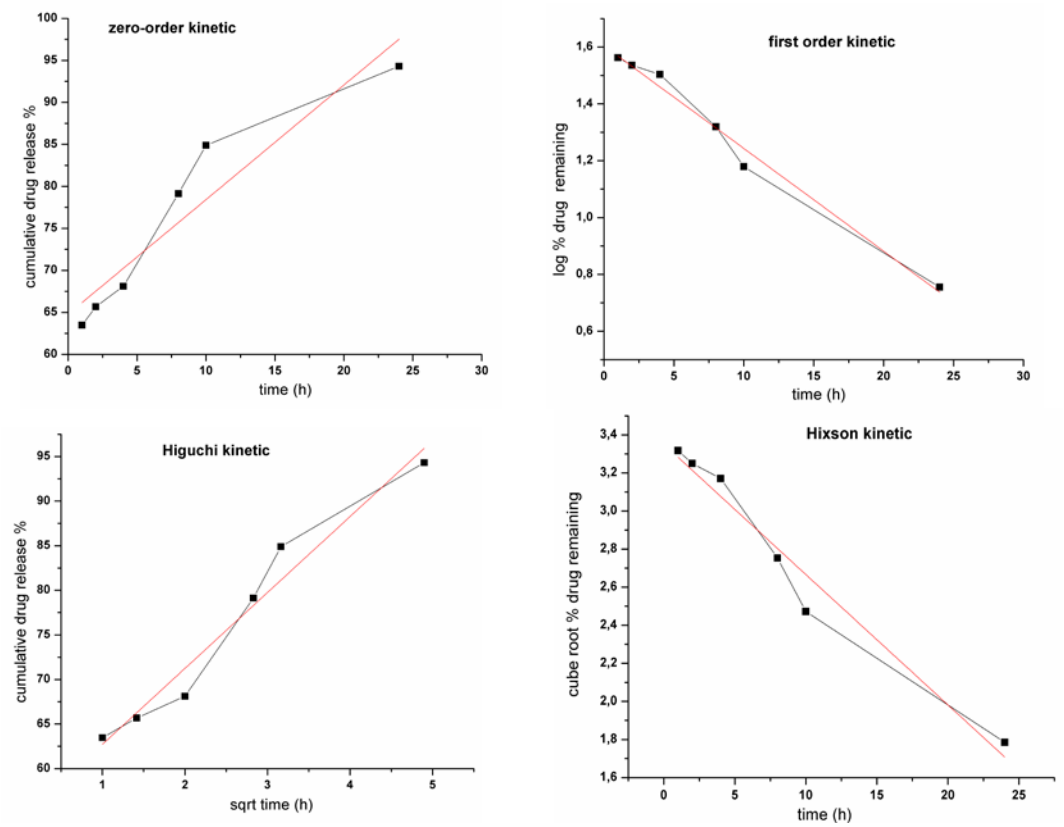

Fig. 5. Best fit kinetic release data of sample N4
experimental data ■ — *linear fits of the data*

Table 3. Values of correlation coefficient for all samples

Sample	Zero order kinetic		First order kinetic		Higuchi model		Korsmeyer-Peppas model		Hixson-Crowell model	
	R^2	K	R^2	K	R^2	K	R^2	n	R^2	K
N4	0.868	1.363	0.983	-0.083	0.953	8.511	-	-	0.958	-0.068
P4	0.756	1.561	0.809	-0.021	0.913	10.102	0.951	0.619	0.792	-0.030
N3	0.776	1.821	0.941	-0.094	0.909	11.652	-	-	0.895	-0.081
P3	0.782	1.617	0.512	-0.028	0.711	12.685	0.950	0.593	0.500	-0.037
N2	0.788	1.877	0.980	-0.083	0.923	12.015	-	-	0.943	-0.076
P2	0.841	2.890	0.809	-0.052	0.869	18.527	0.952	0.840	0.769	-0.066

From the data presented in the table 3 we observe that the correlation coefficients for the zero-order kinetic model are low. The polymeric matrices with drug molecules dissolved or dispersed are matrix-type drug delivery systems. The SA release rate of these systems is time dependent and depends of the initial drug loading and the properties of polymer matrix. Drug release by diffusion of the drug through the polymer matrix and the drug release is not zero-order. The release of SA is associated with the penetration of water into the fibres and the dissolution of drug in water. The smaller the fiber diameter, the shorter the time needed for water to penetrate the fibre. This could be one reason for the high release rate. The burst depletion is probably due to the low compatibility of SA and the PVA polymer, the accumulation of SA on the fibres surface and the small fibres diameter. Due to the initial burst release, none of the models fit the data obtained from this study. From this reason, it could not apply the Korsemeyer-Peppas model to describe the mechanism of drug release. Consequently, the release of SA from PVA matrix follows probably a combination of the first-order model and Higuchi model [20].

The values of release exponent from the Korsemeyer - Peppas model indicates that drug release from the films were non Fickian diffusion. Anomalous transport occurs due to a coupling of Fickian diffusion and polymer relaxation. In the anomalous processes of drug release, Fickian diffusion through the hydrated layers of the matrix and polymer chain relaxation/erosion are both involved.

4. Conclusion

The PVA electrospun fibres and films were obtained from polymer solution. Following the incorporation of SA in PVA matrix as electrospun nanofibres and films was examined by different techniques such as: Attenuated Total Reflectance Fourier Transform Infrared (ATR FTIR) spectroscopy, X-ray photoelectron spectroscopy (XPS), scanning electron microscopy (SEM) measurement and the results were correlated. The changes in shape, size and intensity of peaks in ATR FTIR and XPS spectra have evidenced the surface structure modifications. The investigation related to release of SA revealed that the drug release from polymer samples follows a combination of the kinetics models. Anomalous transport of drug occurs due to a coupling of Fickian diffusion and polymer relaxation. The burst effect observed when salicylic acid was released from the polymer samples could be partly due to higher drug concentration near the surface of the films and fibres.

Acknowledgement

This research was supported by the European Social Fund in Romania, under the responsibility of the Managing Authority for the Sectoral Operational Programme for Human Resources Development 2007-2013 [grants POSDRU/ 6/1.5/S/25].

References

[1] European Pharmacopoeia, V Edition, 2272 (2005).
[2] P. Taepaiboon, U. Rungsardthong, P. Supaphol, Nanotechnology **18**, 175102 (2007).
[3] B. Wang, Y. Wang, T. Yin, Chem. Eng. Comm. **197**, 1315 (2010).
[4] N. Bhardwaj, S. C. Kundu, Biotechnol. Adv. **28**, 325 (2010).
[5] B. Ding, M. Wang, J. Yu, G. Sun, Sensors **9**, 1609 (2009).
[6] S. Singh, S. G. Lakshmi, M. Vijayakumar, Nanobiotechnol. **5**, 10 (2009).
[7] D. H. Reneker, A. L. Yarin, Polymer **49**, 2387 (2008).
[8] S.A. Theron, E. Zussman, A.L.Yarin, Polymer **45**, 2017 (2004).
[9] J. Venugopal, S. Ramakrishna, Appl. Biochem. Biotech. **125**, 147 (2005).
[10] X. Liu, T. Lin, J. Fang et al. J. Biomed. Mater. Res. A. **94A**, 499 (2010).
[11] Z. M. Huang, Y. Z. Zhang, M. Kotaki, S. Ramakrishna, Compos. Sci. Technol. **63**, 2223 (2003).
[12] Q. P. Pham, U. Sharma, A. G. Mikos, Tissue. Eng. **12**, 1197 (2006).
[13] D. H. Song, E. J. Kim, J. P. Kim, Mol. Cryst. Liq. Cryst. **463**, 141 (2007).
[14] E. Beekman, C. Kocher, A. Kokil, J. Appl. Polym. Sci. **86**, 1235 (2002).
[15] J. Sriupayo, P. Supaphol, J. Blackwell, R. Rujiravanit, Polymer. **46**, 5637 (2005).
[16] L. C. Wang, X. G. Chen, D.Y. Zhong, Q. C. Xu, J. Mater. Sci.-Mater. M. **18**, 1125 (2007).
[17] I. Z. Schroeder, P. Franke, U. F. Schaefer, C. M. Lehr, Eur. J. Pharm. Biopharm. **65**, 111 (2007).
[18] O. Sanli,I. Karaca, N. Isiklan, J. Appl. Polym. Sci. **111**, 2731 (2009).
[19] G. Asman, O. Sanli, D. Tuncel, J. Appl. Polym. Sci. **107**, 3291(2008).
[20] I. Michalak, D. Traczyk, M. Mucha, Progress in the Chemistry and Application of Chitin and its Derivatives, **XV**, 107 (2010).
[21] D. Brunelli, T. Atvars, I. Joekes, V. C. Barbosa, J. Appl. Polym. Sci. **69**(4), 645 (1998).

[22] J. M. Gohil, A. Bhattacharya, P. Ray, J. Polym. Res. **13**, 161 (2006).
[23] Z. I. Ali, F. A. Ali, A. M. Hosam, Spectrochim. Acta A. **72**, 868 (2009).
[24] X. S. Feng, M. X. Yu, H. G. Liu et al. Langmuir **16**(24), 9385 (2000).
[25] Pal, K., A. K. Banthia, and D. K. Majumdar, J. Mater. Sci. Mater. Med. **18**, 1889 (2007).
[26] M. A. Helfand, J. B. Mazzanti, M. Fone, R. H. Reamey, Langmuir. **12**, 1296 (1996).
[27] M. Ilčin, O. Hola, B. Bakajová, J. Kučerík, J. Radioanal. Nucl. Ch. **283**, 9 (2010).
[28] M. Abdelaziz, E. M. Abdelrazek, Physica A **390**, 1 (2007).
[29] C. A. Finch, Chemical reactions and stereochemistry of Polyvinyl Alcohol in Polyvinyl Alcohol Devlopments, John Wiley & Sons Ltd. (1992).
[30] M. Kamal Abd El-Kader, J. Appl. Polym. Sci. **88**, 589 (2003).
[31] J. T. Clarke, E. R. Blout, J. Polym. Sci. **1**(5), 419 (1946).
[32] O. Olabisi, Handbook of Thermoplastics. New York: Marcel Dekker, (1997).
[33] X. Huang, C. S. Brazel, J. Control. Release, **73**, 121 (2001).
[34] C. S. Kim, D. M. Saylor et al. J. Biomed. Mater. Res. B, **90B**, 688 (2009).
[35] S. K. Mallapragada, N. A. Peppas, P. Colombo, J. Biomed. Mater. Res. B, **36**, 125 (1997).
[36] X. Huang, C. S. Brazel Chem. Eng. Comm. **190**, 519 (2003).
[37] P. Costa, J. M. S. Lobo, Eur. J. Pharm. Sci. **13**, 123 (2001).